Organic & Biomolecular Chemistry

PAPER

View Article Online
View Journal | View Issue

Cite this: *Org. Biomol. Chem.*, 2014, **12**, 3641

Fluorescent push–pull pH-responsive probes for ratiometric detection of intracellular pH†

Martin Ipuy,[a] Cyrielle Billon,[b] Guillaume Micouin,[a] Jacques Samarut,[b] Chantal Andraud[a] and Yann Bretonnière*[a]

Received 20th January 2014,
Accepted 31st March 2014

DOI: 10.1039/c4ob00147h

www.rsc.org/obc

A family of fluorescent push–pull pH-responsive probes based on 2-dicyanomethylidene-3-cyano-4,5,5-trimethyl-2,5-dihydrofuran as a strong electron acceptor group is described. Small structural variations allow obtaining pK_a ranging from 4.8 to 8.6, underlining the role of the substituent in modulating the acidic properties. Remarkable changes in the optical properties (in particular the fluorescence intensity ratios) were observed as a function of pH. The most interesting probes with pK_a close to neutrality were used for ratiometric imaging of intracellular pH.

Introduction

Phenolic compounds are amongst the most important classes of dyes characterized by acidity of the hydroxy group. The pK_a of phenol is 9.98, but when electron-withdrawing groups that can stabilize the phenoxide ion are present, a substantial change in acidity of the OH group can be noted.[1] For example, the ionization constants of *o*- and *p*-nitrophenol are several hundred times greater than those of phenol with pK_a of 7.23 and 7.15 respectively. Moreover, the hydroxy group OH is a weak electron donating group whereas the deprotonated O^- is a much stronger donating group with a negative charge that can delocalize along a conjugated path. As a consequence, the phenol and the corresponding phenolate ion display very different optical properties in absorption and emission, with the latter being usually much more emissive. This unique feature has been intensively exploited in the design of fluorescent indicators for intracellular pH.[2] Most of the pH indicators developed so far (Fig. 1), such as 1,4-DHPN (1,4-dihydroxyphthalonitrile),[3] HPTS (1-hydroxypyrene-3,6,8-trisulfonate),[4] BCECF (2′,7′-bis-(2-carboxyethyl)-5-(and-6-)carboxyfluorescein),[5] or the long-wavelength fluorescent SNAFL (seminaphthofluoresceins),[6] SNAFR (seminaphthofluorones),[7] and SNARF (seminaphthorhodafluors),[8] are phenol derivatives spanning the physiological pH from different organelles (4.50–6.00 range) to the cytosol (6.80–7.40 range) and covering a wide range of absorption and emission wavelengths. These indicators are often used as ratiometric (or dual) excitation or emission pH indicators because the absorption or emission profile of the fluorophore changes significantly with the pH. Given the importance of modulating the pK_a of phenol derivatives, finding new simple fluorescent structures containing a phenol group is of prime interest.

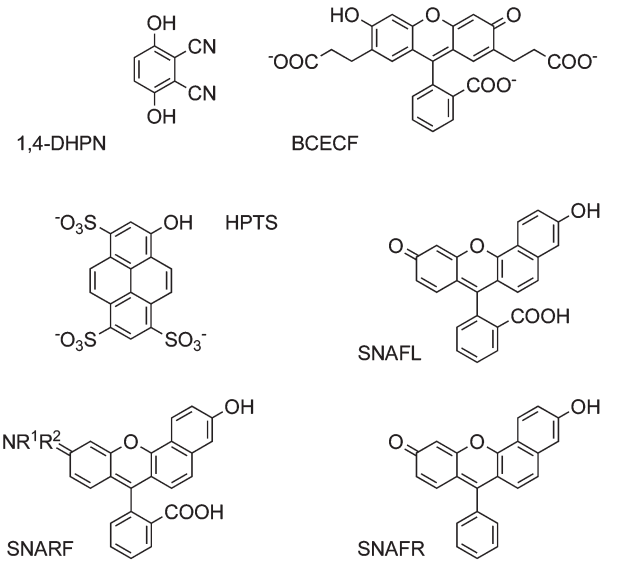

Fig. 1 Examples of commonly used phenol-based pH sensitive fluorophores.

2-Dicyanomethylidene-3-cyano-4,5,5-trimethyl-2,5-dihydrofuran (TCF) is a strong electron-withdrawing group that has been extensively used in the design of highly active nonlinear

[a]*Laboratoire de Chimie de l'ENS de Lyon, CNRS UMR 5182, Ecole Normale Supérieure de Lyon, Université Lyon I, 46 allée d'Italie, 69364 Lyon cedex 07, France. E-mail: yann.bretonniere@ens-lyon.fr; Fax: +33-4-7272-8860; Tel: +33-4-7272-8399*
[b]*Institut de Génomique Fonctionnelle de Lyon, Université de Lyon, Université Lyon 1, CNRS, INRA, Ecole Normale Supérieure de Lyon, 46 allée d'Italie, 69364 Lyon cedex 07, France*

†Electronic supplementary information (ESI) available: Includes additional figures, full spectroscopic properties of compounds **2a–2j** and complete NMR data for compounds **2a–2j**. See DOI: 10.1039/c4ob00147h

optical materials.[9] In comparison, only very few examples described its use in the design of red fluorescent probes for bioimaging, only in combination with *N*,*N*-dialkylanilino groups as electron-donating groups.[10] Strong absorption, relatively high fluorescence quantum yield, and sensitivity of their fluorescence to the local environment make them interesting for single molecule imaging,[10a,e] pH,[11] thiol[10d] or K^+ sensors.[10f] TCF dyes containing other electron-donating groups such as methoxy have seldom been described. And yet, besides their highly environment sensitive optical properties, they have been shown to be more photostable than their *N*,*N*-dialkylanilino equivalents.[12] In this article we report the design, synthesis and study of the physical and optical properties of a new series of simple push–pull dipolar phenol derivatives **2a–2j** (Scheme 1) containing the 2-dicyanomethylidene-3-cyano-4,5,5-trimethyl-2,5-dihydrofuran (TCF) ring. These pH responsive dyes are fluorescent in both the acidic (neutral) and the basic (anionic) form and behave as selective fluorescent pH receptors in aqueous solutions.

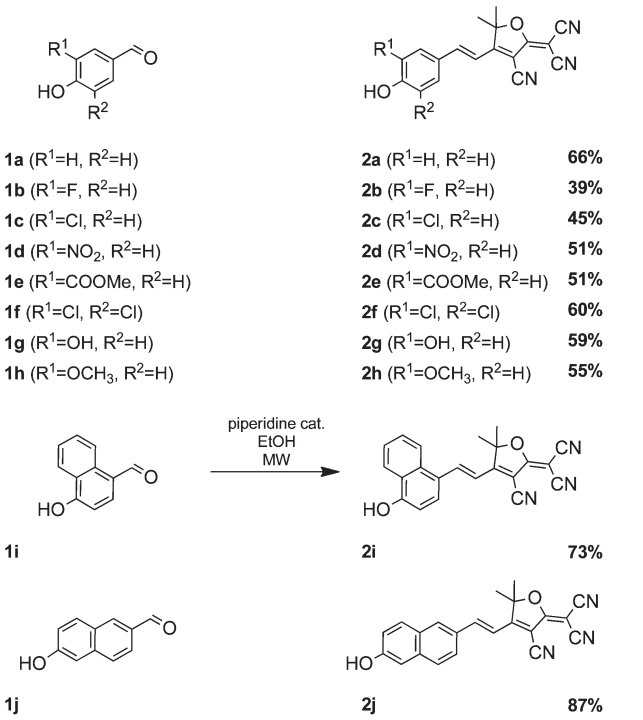

1a (R^1=H, R^2=H) **2a** (R^1=H, R^2=H) 66%
1b (R^1=F, R^2=H) **2b** (R^1=F, R^2=H) 39%
1c (R^1=Cl, R^2=H) **2c** (R^1=Cl, R^2=H) 45%
1d (R^1=NO_2, R^2=H) **2d** (R^1=NO_2, R^2=H) 51%
1e (R^1=COOMe, R^2=H) **2e** (R^1=COOMe, R^2=H) 51%
1f (R^1=Cl, R^2=Cl) **2f** (R^1=Cl, R^2=Cl) 60%
1g (R^1=OH, R^2=H) **2g** (R^1=OH, R^2=H) 59%
1h (R^1=OCH_3, R^2=H) **2h** (R^1=OCH_3, R^2=H) 55%

1i **2i** 73%

1j **2j** 87%

Scheme 1 Synthesis of compounds **2a–2j**.

Results and discussion

The synthesis of **2a–g** (Scheme 1) involved a simple Knoevenagel condensation between TCF and the corresponding aldehyde. This reaction was performed by controlled microwave irradiation in ethanol and in the presence of piperidine as a catalyst. The synthesis of TCF derivatives by microwave heating is well established and has been shown to give a better yield than traditional heating.[13] Using this simple procedure allowed recovering the compounds by simple filtration from the reaction mixture in average to good yields (39 to 87%).

Table 1 contains the spectroscopic data for compounds **2a–2i**. The absorption spectra of **2a–2j** in DMSO–water mixtures (1/5 v/v) at low pH where only the phenol forms are present display a broad band characteristic of a charge transfer transition. Absorption maxima ranged from 414 nm for **2d** to 512 nm for **2i**. When compared to the simplest compound **2a**, introducing an electron-withdrawing group in the *ortho* position with respect to that of the phenol induced a hypsochromic shift in the absorption maxima (up to 34 nm for the nitro group in **2d**). However, elongation of the conjugated path (**2i–2j**) or introduction of the electron-donating group in the *ortho* position (**2g–2h**) was characterized by a bathochromic shift in the absorption maximum wavelength (up to 64 nm for compound **2i**).

The dramatic changes in the absorption spectra (Fig. 2a and 3a) observed when the pH is increased accounted for the formation of the phenoxide at higher pH (Scheme 2). The band centred around 460 nm gradually decreased and a new narrow absorption peak appeared whose maximum was

Table 1 Spectroscopic properties of compounds **2a–2j**

	Neutral form				Phenoxide			
	λ_{abs} (ε)[a] nm (L mol^{-1} cm^{-1})	λ_{em}[a] nm	$\Delta\lambda$[c] nm	Φ[d] ($\varepsilon\Phi$)	λ_{abs} (ε)[b] nm (L mol^{-1} cm^{-1})	λ_{em}[b]	$\Delta\lambda$[c] nm	Φ[e] ($\varepsilon\Phi$)
2a	448 (48 500)	563	115	0.011 (530)	588 (181 000)	614	26	0.002 (360)
2b	436 (39 400)	565	129	0.017 (670)	586 (238 000)	618	32	0.004 (950)
2c	438 (44 000)	560	122	0.015 (660)	584 (234 000)	619	35	0.007 (1640)
2d	414 (60 000)	542	128	0.015 (900)	537 (203 000)	614	77	0.053 (10 760)
2e	428 (43 200)	550	122	0.005 (215)	570 (201 000)	611	41	0.012 (2410)
2f	423 (31 600)	—	—	—	574 (254 000)	626	52	0.012 (3050)
2g	465 (56 600)	595	130	0.01 (570)	605 (165 000)	650	45	<0.005 (<825)
2h	462 (60 800)	598	136	0.05 (3040)	610 (134 000)	644	34	<0.002 (<270)
2i	512 (52 300)	634	122	0.035 (1830)	632 (101 000)	655	23	0.003 (300)
2j	465 (51 500)	648	183	0.099 (5100)	—	—	—	—

[a] In water at pH = 2. [b] In water at pH = 10. λ_{exc} was set at the wavelength of the isosbestic point of the absorption-based pH titration. [c] Stokes shift. [d] Measured in DMSO using Coumarin 153 in methanol (Φ = 0.54) as the reference. [e] Measured in DMSO using cresyl violet in methanol (Φ = 0.57) as the reference.

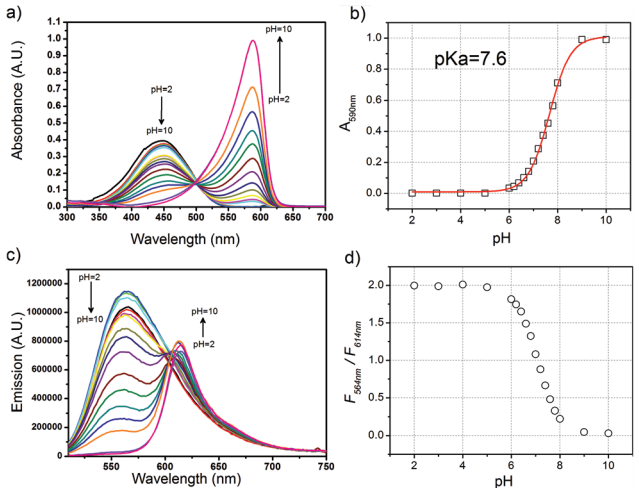

Fig. 2 (a) Absorption spectra of **2a** at different pH values in HEPES buffer. (b) Changes of the absorbance at 590 nm ($A_{590\ nm}$) over the pH range 2–10 with non-linear least-square fit of the experimental data. (c) Emission spectra of **2a** at different pH in HEPES buffer (λ_{exc} = 500 nm). (d) Emission intensity ratio changes ($F_{554\ nm}/F_{614\ nm}$) over the pH range 2–10.

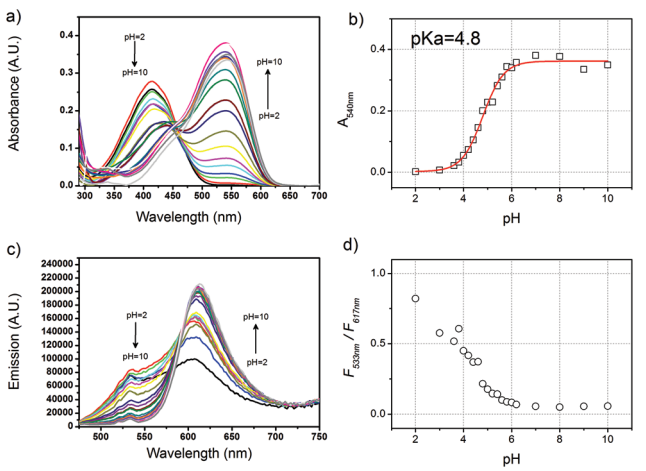

Fig. 3 (a) Absorption spectra of **2d** at different pH in HEPES buffer. (b) Changes of the absorbance at 540 nm ($A_{540\ nm}$) over the pH range 2–10 with non-linear least-square fit of the experimental data. (c) Emission spectra of **2d** at different pH in HEPES buffer (λ_{exc} = 455 nm). (d) Emission intensity ratio change ($F_{533\ nm}/F_{617\ nm}$) over the pH range 2–10.

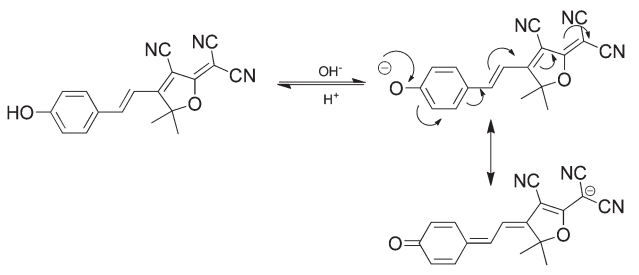

Scheme 2 pH modulated switching of **2a**.

considerably red-shifted compared to the neutral form. The absorption maxima now ranged from 537 nm for **2d**, 588 nm for the simplest compound **2a** up to 632 nm for **2i** with a naphthalene ring. The two bands interconverted with an isosbestic point. The influence of the substituent on the absorption of the phenoxides was less pronounced than that for the neutral forms. Based on the absorption of **2a** only small hypsochromic shifts were observed. It has to be noted that for all compounds the molar absorption coefficient of the deprotonated form was much higher (around 5 times) than the protonated form (Table 1). The switch between the phenol and the phenoxide (Scheme 2) was fully reversible. The absorption of the phenol re-appeared upon re-acidification of the solution and no noticeable changes in the absorption of **2a** could be observed after 10 cycles between pH = 4 and pH = 10. ^{1}H NMR experiments confirmed the reversibility of the proton exchange (see ESI†).

Recording the absorption at various pH values enabled determining the pK_a values of all compounds by fitting by non-linear regression the sigmoid response of absorption value *vs.* pH according to eqn (1):

$$A = \frac{K_a \times A_F + 10^{-pH} \times A_0}{K_a + 10^{-pH}} \quad (1)$$

where A_F and A_0 are respectively the final (high pH) and the initial (low pH) absorption. The pK_a values obtained (Table 2) varied from 4.2 for **2f** to 8.9 for **2j**, spanning the intracellular pH range. As expected, installation of the electro-withdrawing group *ortho* to the hydroxy group induced a decrease of the pK_a value,[14] the nitro substituted compound **2d** being almost 1000 times more acidic than the parent **2a**. Surprisingly, introduction of the OR (OH and OCH_3) electro-donating group *ortho* to the hydroxy group also induced a small decrease in the pK_a probably due to the inductive withdrawing effect of the O atom. Indeed a good correlation was found when plotting the pK_a value of all phenyl compounds (*i.e.* **2a–2h**, Fig. 4) *vs.* the Hammet σ_m value (Table 2) characteristic of the inductive effect of the substituent.[15] The deviation observed for com-

Table 2 Hammett σ_m constant, pK_a and the excited state pK_a^* of compounds **2a–2j**

	Substituent group	σ_m [a]	pK_a [b]	pK_a^* [c]
2a	H	0	7.6	0.5
2b	F	0.34	6.4	−1.3
2c	Cl	0.37	6.0	−1.8
2d	NO_2	0.71	4.8	−3.3
2e	COOMe	0.37	7.2	−0.8
2f	Cl, Cl	0.74	4.2	—
2g	OH	0.12	6.9	0.2
2h	OCH_3	0.12	7.1	0.3
2i	—	—	5.3	0.9
2j	—	—	8.9	—

[a] Substituent inductive value taken from ref. 15. [b] Values obtained from eqn (1) by non-linear least-square fitting of experimental data. [c] Values calculated according to eqn (2) and the experimental data from Table 1.

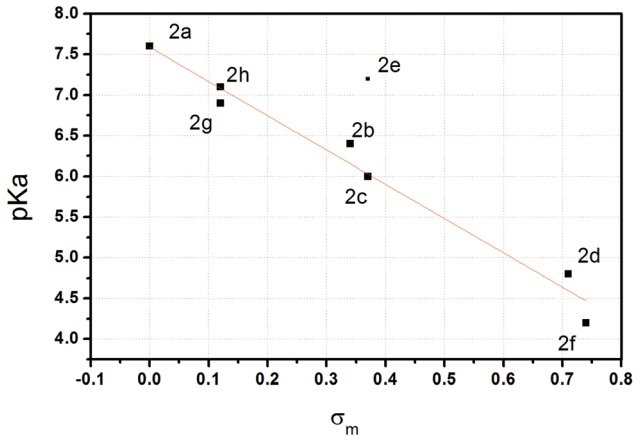

Fig. 4 Plot of pK_a as a function of σ_m for phenyl compounds **2a–2h** showing good correlation between the pK_a value and the inductive effect of the substituent. The solid line is the linear fit (r = 0.971).

pound **2e** bearing an ester group can be explained by the presence of a five member hydrogen bonding between the OH group and the C=O bond of the ester that stabilizes the phenol and decreases its acidity.

The fluorescence properties of all compounds were also studied in water: first at low pH, where only the neutral form was present, and then the pH was increased. Significant differences were observed, depending on the nature of the substituent group. For the four compounds having the highest pK_a (**2a**, **2g**, **2h** and **2j**), as well as **2i**, low pH excitation at the wavelength of the isosbestic point of the absorption-based pH titration gave rise to a single emission (Fig. 2c, and SI-5 to SI-8†) attributed to the phenol. This emission was characterized by a large band with a red shift in the maxima and a large Stokes' shift increasing from 115 nm for **2a** up to 183 nm for **2j** with the presence of an *ortho*-electron-donating group. When the pH was increased, the emission of the phenoxide appeared as a narrow band with a small Stokes' shift. The only exception was **2j** for which the phenoxide was hardly fluorescent. The introduction of an electron donating group *ortho* to the phenol induced a considerable red shift in the emission of the phenoxide (up to 40 nm for **2g**).

For the other compounds with lower pK_a (*i.e.* **2b–2f**), excitation of the neutral form at low pH resulted in dual emission of phenol and phenoxide (Fig. 3c, and SI-1 to SI-4†). The emission of the phenol was also characterized by a large band and a large Stokes' shift, whereas the emission of the phenoxide ion was narrow and displayed a smaller Stokes' shift. The presence of an electron-withdrawing group *ortho* to the phenol induced a blue shift in the emission maxima of the phenol compared to **2a**, but a small increase in the Stokes' shift.

Contrary to what was recently reported for other phenol based fluorophores,[16] for which two inflexion points corresponding to the ground state pK_a and the excited state pK_a (pK_a^*) were observed, for all compounds **2a–2j** a plot of the maximum intensities *vs.* pH displayed only one inflexion point (data not shown). Fitting gave pK_a values close to what was obtained by fitting the absorption data. This is surprising because estimation of the excited state pK_a (pK_a^*, Table 2) using the Förster cycle equation[17] (2):

$$pK_a - pK_a^* = \frac{hc\left(\tilde{\nu}_{Abs}^{ArOH} - \tilde{\nu}_{Abs}^{ArO^-} + \tilde{\nu}_{Em}^{ArOH} - \tilde{\nu}_{Em}^{ArO^-}\right)}{2(2.303kT)} \quad (2)$$

where the terms $\tilde{\nu}$ represent the energy of the electronic transitions for the species ArOH and ArO^- respectively, obtained from the maxima of the absorption and emission spectra at low and high pH given in Table 1, clearly differentiated strong photoacids (with pK_a^* < 0 for **2b–2e**) and weaker photoacids (pK_a^* > 0 for **2a**, **2g–2i**).

For all compounds, with the notable exception of **2d**, the fluorescence quantum yield of the neutral form was higher than that of the anionic form. The fluorescence quantum yields are rather low (the maximum is for **2j** with 9.9%), but the overall brilliance $\varepsilon\Phi$ of these objects reaches 500 to 4000 L mol^{-1} cm^{-1}. Moreover, the study of the variation of fluorescence or fluorescence intensity ratios as a function of pH showed a good response around physiological pH, especially for probes **2a**, **2g** and **2h**. With an excitation at the wavelength of the isosbestic point, large ratio increases of the fluorescence intensity ratios R ($R_{pH=2}/R_{pH=8}$ = 70 for the best compound **2a**) were determined between the two extreme pH values. As shown in Fig. 2d and 3d, the highest variation occurs around pH = 7, indicating that these dyes are well suited for imaging of intracellular pH with a ratiometric response in emission.

To determine whether these new dyes can be used in intracellular pH imaging, preliminary experiments were carried out with probes **2a** and **2g** using laser confocal scanning microscopy. These probes were excited at 488 nm or 514 nm respectively with an argon ion laser and showed well separated emissions from the protonated and deprotonated forms of the fluorophores for ratiometric emission experiments. Specifically, HeLa cells were incubated with 1 μM compound **2a** (resp. **2g**) for 5 minutes. Good quality images were obtained upon excitation at 488 nm (resp. 514 nm) revealing that the two probes enter the cells immediately after loading (Fig. 5). Bright-field transmission measurements after dye incubation confirmed that the cells were viable. At physiological pH (pH = 7.4), the fluorescence could be detected in the green (500/550 nm for **2a** and 535/590 nm for **2g**) and the red (600/650 nm for **2a** and 650/710 nm for **2g** resp.) emission chan-

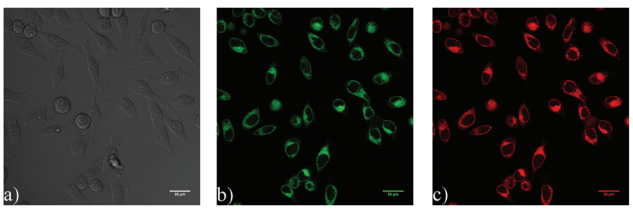

Fig. 5 Confocal images of HeLa cells incubated at pH = 7.4 and with 1 μM **2a** for 5 minutes at 37 °C (λ_{exc} = 488 nm): (a) bright field; (b) green emission channel (500–550 nm); (c) red emission channel (600–650 nm); scale bar: 25 μm.

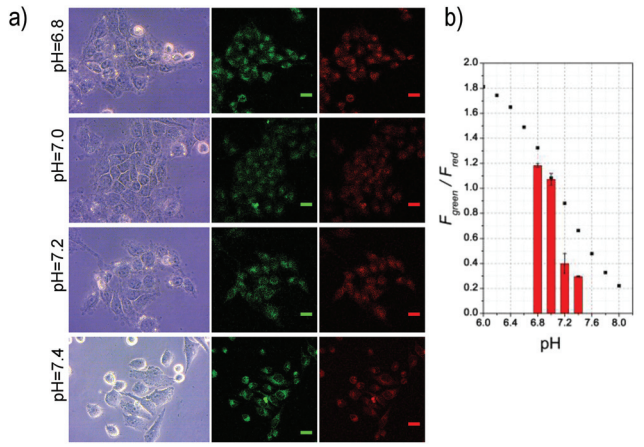

Fig. 6 (a) Confocal images of HeLa cells incubated at different pH and with 1 μM **2a** for 5 minutes at 37 °C (λ_{exc} = 488 nm). From left to right: bright field, green emission channel (500–550 nm), red emission channel (600–650 nm); scale bar: 25 μm. (b) Evolution of the emission ratio $R = F_{green}/F_{red}$ as a function of pH. The black squares represent the emission ratio $F_{554\ nm}/F_{614\ nm}$ obtained from the titration (Fig. 1d).

nels, proving that the two forms exist in agreement with the measured pK_a. We then applied **2a** and **2g** to HeLa cells grown at different pH values (6.8 to 7.4) to observe the changes in fluorescence on the two channels. Bright-field transmission images confirmed the viability of cells after incubation even at lower pH (Fig. 6). Different areas of interest (ROI) were defined. The fluorescence intensity in the two channels in those ROI was measured to give the values of F_{green} and F_{red}. Similarly, fluorescence intensity ratios $R = F_{green}/F_{red}$ of 4 for **2a** and 2.7 for **2g** were obtained between pH = 6.8 and pH = 7.4 (Fig. 6b and SI-9†) closely matching the values obtained in solution (Fig. 2 and SI-5†). The data showed that these new probes strongly depend on pH and could distinguish near-neutral minor pH fluctuations in cells.

Conclusions

In conclusion, we developed a family of fluorescent push–pull pH-responsive probes based on TCF as a strong electron acceptor group. Small structural variations allowed fine tuning of the pK_a between 4.8 and 8.9. In aqueous solution, the fluorescence showed remarkable changes in ratiometric response to small pH variations around neutrality with large emission shifts. The simple structure of these fluorophores allows further chemical functionalization for the targeting of specific subcellular compartments. Compound **2h**, in particular, having a pK_a of 7.1 and a methoxy group that can easily be modified, looks rather interesting in that view.

Experimental section

Commercially available materials were used as received. Analytical thin-layer chromatography (TLC) was carried out on a Merck 60 F_{254} precoated silica gel plate (0.2 mm thickness). Visualization was performed using a UV lamp. Microwave syntheses were conducted in a 20 mL sealed tube on a Biotage Initiator 2.5 single-mode reactor using external IR temperature control. TCF (2-dicyanomethylidene-3-cyano-4,5,5-trimethyl-2,5-dihydrofuran) was synthesized according to a literature procedure.[18] Melting points were recorded on a differential scanning calorimeter operating between 30 and 400 °C. NMR spectra were recorded at ambient temperature on a standard spectrometer operating at 500 MHz for ^{1}H and 125 MHz for ^{13}C. Chemical shifts are given in parts per million (δ/ppm) and are reported relative to tetramethylsilane (^{1}H, ^{13}C) using the residual solvent peaks as the internal standard. ^{1}H NMR splitting patterns are designated as singlet (s), doublet (d), triplet (t), quartet (q), dd (doublet of doublets) or m (multiplets). Infrared spectra (IR) were recorded on a FT-IR spectrophotometer and are reported as wavelength numbers (ν/cm^{-1}). Low resolution mass spectra were taken on a LC-MS instrument and high resolution mass spectra (HRMS) were recorded on an IF-TOF spectrometer.

Spectroscopy

Absorption spectra (UV-Vis) were recorded on a dual beam Jasco 670 spectrometer. Data are reported as absorption maximum wavelength (λ_{max}/nm) and molar extinction coefficient at the absorption maximum wavelength (ε/L mol^{-1} cm^{-1}). Fluorescence spectra were performed on a Horiba Jobin-Yvon Fluorolog-3® spectrofluorimeter equipped with a red-sensitive Hamamatsu R928 photomultiplier tube. Spectra were reference corrected for both the excitation source light intensity variation (lamp and grating) and the emission spectral response (detector and grating).

Fluorescence quantum yields Φ were measured in diluted water solutions. Coumarin-153 in methanol (Φ = 0.54)[19] or Cresyl Violet in methanol (Φ = 0.57)[19] were used as the reference for the emission range 500–700 nm and 575–750 nm respectively. The sample and the reference are excited at the same wavelength (λ_{exc}). The quantum yield relative to the reference is given by eqn (3):

$$\Phi^S = \Phi^{Ref} \frac{S^S}{S^{Ref}} \times \left(\frac{n_d^S}{n_d^{Ref}}\right)^2 \quad (3)$$

where S is the slope obtained by plotting the integrated area under the fluorescence emission spectrum *vs.* the absorbance at λ_{exc} and n_d is the refractive index of the solvents. Superscripts Ref and S correspond to the reference and the sample respectively. For each experiment 5 points were recorded, all corresponding to an absorbance at λ_{exc} below 0.1.

General procedure for the Knoevenagel reaction

The aldehyde **1** (1 mmol) and TCF (1.15 mmol, 230 mg) were dissolved in 10 mL of anhydrous ethanol in a 20 mL microwave vial. 2 drops of piperidine were added. The vial was sealed with a pressure septum and the mixture was irradiated by focused microwaves at 100 °C for 15 minutes by controlling

the temperature. After cooling, the precipitate was filtered off and washed with ethanol and cyclohexane to give the pure desired product.

2a. Yield: 66% (200 mg), orange solid. m.p. >260 °C. ^{1}H NMR (500 MHz, DMSO-d_6): δ/ppm 10.57 (s, 1 H, OH), 7.86 (d, 1 H, J = 16.4 Hz), 7.77 (d, 2 H, J = 8.4 Hz), 6.98 (d, 1 H, J = 16.4 Hz), 6.86 (d, 1 H, J = 8.4 Hz), 1.74 (s, 6 H, –CH_3). ^{13}C NMR (125 MHz, DMSO-d_6): δ/ppm 177.9, 176.5, 162.9, 148.9, 132.9 (2 C), 126.3, 117.0 (2 C), 113.5, 112.7, 112.3, 111.8, 99.6, 97.3, 53.8, 25.9 (2 C). Elemental analysis calcd for $C_{18}H_{13}N_3O_2$: C 71.28, H 4.32, N 13.85; found: C 71.92, H 4.46, N 13.88. MS (ES$^-$): m/z 302.0 for [M − H]$^-$. IR (KBr): ν/cm^{-1} 3366, 2224, 1554, 1524, 1380, 1281, 1211, 1162.

2b. Yield: 39% (125 mg), brown solid. m.p. >260 °C. ^{1}H NMR (500 MHz, DMSO-d_6): δ/ppm 11.02 (s, 1 H, –OH), 7.89 (dd, 1 H, J = 12.6 Hz, J = 1.5 Hz), 7.85 (d, 1 H, J = 16.3 Hz), 7.58 (dd, 1 H, J = 8.4 Hz, J = 1.5 Hz), 7.08 (d, 1 H, J = 16.3 Hz), 7.05 (t, 1 H, J = 8.4 Hz), 1.77 (s, 6 H). ^{13}C NMR (125 MHz, DMSO-d_6): δ/ppm 177.8, 175.9, 151.5 (d, 1 C, J_{C-F} = 240 Hz), 150.5 (d, 1 C, J_{C-F} = 15 Hz), 147.5, 128.8, 126.8 (d, 1 C, J_{C-F}= 7 Hz), 118.8 (d, 1 C, J_{C-F} = 5 Hz), 117.3 (d, 1 C, J_{C-F} = 18 Hz), 113.7, 113.4, 112.6, 111.7, 99.7, 97.9, 54.2, 25.8 (2 C). Elemental analysis calcd for $C_{18}H_{12}FN_3O_2$: C, 67.29; H, 3.76; N, 13.08; found: C 67.28; H 4.10; N 13.00. MS (ES$^-$): m/z 320.0 (100%), 321.0 (20.6%) for [M − H]$^-$. IR (KBr): ν/cm^{-1} 3420, 2222, 1563, 1531, 1516, 1300, 1282, 1180, 1165, 1101.

2c. Yield: 45% (150 mg), orange solid. m.p. >260 °C. ^{1}H NMR (500 MHz, DMSO-d_6): δ/ppm 11.28 (s, 1 H, –OH), 8.03 (d, 1 H, J = 1.5 Hz), 7.80 (d, 1 H, J = 16.0 Hz), 7.70 (dd, 1 H, J = 8.4 Hz, J = 1.5 Hz), 7.05 (d, 1 H, J = 16.0 Hz), 7.03 (d, 1 H, J = 8.4 Hz), 1.74 (s, 6 H, –CH_3). ^{13}C NMR (125 MHz, DMSO-d_6): δ/ppm 177.8, 176.1, 157.7, 147.2, 132.2, 130.8, 127.4, 121.5, 117.7, 113.8, 113.4, 112.6, 111.6, 99.8, 98.4, 54.4, 25.8 (2 C). Elemental analysis calcd for $C_{18}H_{12}ClN_3O_2$: C 64.01, H 3.58, N 12.44; found: C 64.18, H 3.69, N 12.11. MS (ES$^-$): m/z 336.0 (100%), 337.0 (19%), 338.0 (30%) for [M − H]$^-$. IR (KBr): ν/cm^{-1} 3307, 2237, 2225, 1556, 1513, 1414, 1385, 1298, 1278.

2d. Yield: 51% (178 mg), brown solid. m.p. >260 °C. ^{1}H NMR (500 MHz, DMSO-d_6): δ/ppm 11.96 (s, 1 H, –OH), 8.50 (d, 1 H, J = 1.8 Hz), 8.08 (dd, 1 H, J = 9.0 Hz, J = 1.8 Hz), 7.86 (d, 1 H, J = 16.6 Hz), 7.16 (d, 1 H, J = 9.0 Hz), 7.12 (d, 1 H, J = 16.6 Hz), 1.76 (s, 6 H, –CH_3). ^{13}C NMR (125 MHz, DMSO-d_6): δ/ppm 177.6, 175.6, 155.9, 146.1, 138.2, 135.2, 128.3, 126.1, 120.6, 115.0, 113.3, 112.5, 111.3, 99.9, 99.6, 54.7, 25.8. Elemental analysis calcd for $C_{18}H_{12}N_4O_4$: C 62.07, H 3.47, N 16.09; found: C 61.92, H 3.62, N 16.11. MS (ES$^-$): m/z 347.0 for [M − H]$^-$. IR (KBr): ν/cm^{-1} 3257, 2233, 1579, 1544, 1531, 1311, 1168.

2e. Yield: 51% (184 mg), red solid. m.p. >260 °C. ^{1}H NMR (500 MHz, DMSO-d_6): δ/ppm 11.12 (s, 1 H, –OH), 8.29 (d, 1 H, J = 2.3 Hz), 8.15 (dd, 1 H, J = 8.4 Hz, J = 2.3 Hz), 7.94 (d, 1 H, J = 16.5 Hz), 7.12 (d, 1 H, J = 16.5 Hz,), 7.11 (d, 1 H, J = 8.4 Hz), 3.92 (s, 3 H, –O–CH_3), 1.80 (s, 6 H, –CH_3). ^{13}C NMR (125 MHz, DMSO-d_6): δ/ppm 177.7, 176.1, 168.4, 163.2, 147.2, 135.1, 134.5, 126.6, 119.4, 114.1, 115.6, 113.3, 112.5, 111.5, 99.9, 99.1, 54.5, 53.2, 25.8 (2 C). Elemental analysis calcd for $C_{20}H_{15}N_3O_4$: C 66.48, H 4.18, N 11.63; found: C 65.95, H 4.23, N 11.71. MS (ES$^-$): m/z 360.1 for [M − H]$^-$. IR (KBr): ν/cm^{-1} 3448, 3235, 2231, 2215, 1685, 1575, 1529, 1319, 1216.

2f. Yield: 60% (223 mg), orange solid. m.p. >260 °C. ^{1}H NMR (500 MHz, DMSO-d_6): δ/ppm 8.08 (s, 2 H), 7.76 (d, 1 H, J = 16.6 Hz), 7.21 (d, 1 H, J = 16.6 Hz), 1.77 (s, 6 H, –CH_3). ^{13}C NMR (125 MHz, DMSO-d_6): δ/ppm 177.7, 175.5, 145.5, 130.5 (2 C), 127.9, 123.4 (2 C), 115.4, 113.3, 112.8, 112.5, 111.3, 101.9, 99.8, 54.8, 25.7 (2 C). Elemental analysis calcd for $C_{18}H_{11}Cl_2N_3O_2$: C 58.08, H 2.98, N 11.29; found: C 57.92; H 3.45; N 11.22. MS (ES$^-$): m/z 370.0 (100%), 371.0 (19%), 372.0 (67%) for [M − H]$^-$. IR (KBr): ν/cm^{-1} 3364, 2233, 2212, 1573, 1561, 1525, 1411, 1286.

2g. Yield: 59% (188 mg), dark red solid. m.p. >260 °C. ^{1}H NMR (500 MHz, DMSO-d_6): δ/ppm 10.26 (s, 1 H), 9.46 (s, 1 H), 7.83 (d, 1 H, J = 16.2 Hz), 7.31 (d, 1 H, J = 2.0 Hz), 7.28 (dd, 1 H, J = 8.0 Hz, J = 2.0 Hz), 6.90 (d, 1 H, J = 16.2 Hz), 6.86 (d, 1 H, J = 8.0 Hz), 1.77 (s, 6 H, –CH_3). ^{13}C NMR (125 MHz, DMSO-d_6): δ/ppm 177.8, 176.3, 152.1, 149.3, 146.7, 126.8, 125.4, 116.8, 115.6, 113.6, 112.7, 112.1, 111.9, 99.5, 97.0, 53.5, 25.9 (2 C). Elemental analysis calcd for $C_{18}H_{13}N_3O_3$: C 67.71, H 4.10, N 13.16; found: C 67.60, H 4.11, N 13.15. MS (ES$^-$): m/z 318.0 [M − H]$^-$. IR (KBr): ν/cm^{-1} 3444, 3324, 2242, 2224, 1572, 1519, 1444, 1287, 1192, 1149.

2h. Yield: 55% (183 mg), brown solid. m.p. >260 °C. ^{1}H NMR (500 MHz, DMSO-d_6): δ/ppm 10.30 (s, 1 H), 7.88 (d, 1 H, J = 16.2 Hz), 7.50 (s, 1 H), 7.42 (d, 1 H, J = 8.2 Hz), 7.04 (d, 1 H, J = 16.2 Hz), 6.90 (d, 1 H, J = 8.2 Hz), 3.87 (s, 1 H, –OCH_3), 1.79 (s, 6 H, –CH_3). ^{13}C NMR (125 MHz, DMSO-d_6): δ/ppm 177.9, 176.4, 152.7, 149.4, 148.8, 126.8, 126.1, 116.7, 113.5, 113.3, 112.7, 112.5, 111.8, 99.6, 96.9, 56.4, 53.7, 25.9 (2 C). Elemental analysis calcd for $C_{19}H_{15}N_3O_3$: C 68.46, H 4.54, N 12.61; found: C 68.81, H 4.66, N 12.65. MS (ES$^-$): m/z 332.1 for [M − H]$^-$. IR (KBr): ν/cm^{-1} 3405, 2224, 1568, 1506, 1437, 1301, 1287.

2i. Yield: 73% (258 mg), violet solid. m.p. >260 °C. ^{1}H NMR (500 MHz, DMSO-d_6): δ/ppm 11.56 (s, 1 H, –OH), 8.84 (d, 1 H, J = 15.8 Hz), 8.34 (d, 1 H, J = 8.4 Hz), 8.26 (d, 1 H, J = 7.8 Hz), 8.22 (d, 1 H, J = 7.8 Hz), 7.72 (t, 1 H, J = 7.8 Hz), 7.58 (t, 1 H, J = 7.8 Hz), 7.22 (d, 1 H, J = 15.8 Hz), 7.07 (d, 1 H, J = 8.4 Hz), 1.80 (s, 6 H, –CH_3). ^{13}C NMR (125 MHz, DMSO-d_6): δ/ppm 178.1, 176.3, 160.3, 144.0, 133.8, 130.5, 129.4, 126.2, 125.1, 123.8, 122.8, 122.0, 113.7, 113.3, 112.9, 112.8, 110.2, 99.6, 95.3, 53.4, 25.7 (2 C). Elemental analysis calcd for $C_{22}H_{15}N_3O_2$: C 74.68, H 4.28, N 11.89; found: C 73.62, H 4.41, N 11.97. MS (ES$^-$): m/z 352.1 for [M − H]$^-$. IR (KBr): ν/cm^{-1} 3280, 2228, 2209, 1540, 1510, 1377, 1354, 1262, 1218, 1189.

2j. Yield: 87% (307 mg), brown solid. m.p. >260 °C. ^{1}H NMR (500 MHz, DMSO-d_6): δ/ppm 10.27 (s, 1 H, –OH), 8.27 (s, 1 H), 8.05 (d, 1 H, J = 16.4 Hz), 7.92 (d, 1 H, J = 8.6 Hz), 7.86 (d, 1 H, J = 8.7 Hz), 7.75 (d, 1 H, J = 8.6 Hz), 7.21 (d, 1 H, J = 16.4 Hz) 7.15 (d, 1 H, J = 2.5 Hz), 7.13 (dd, 1 H, J = 8.7 Hz, J = 2.5 Hz), 1.78 (s, 6 H, –CH_3). ^{13}C NMR (125 MHz, DMSO-d_6): δ/ppm 177.8, 176.0, 158.8, 148.8, 137.4, 133.7, 131.8, 129.6, 127.9, 127.8, 124.6, 120.3, 114.4, 113.4, 112.6, 111.8, 109.9, 99.9, 98.3, 54.2, 25.7 (2 C). Elemental analysis calcd for

$C_{22}H_{15}N_3O_2$: C 74.68, H 4.28, N 11.89; found: C 73.92, H 4.30, N 11.73. MS (ES^-): m/z 352.1 for $[M - H]^-$. IR (KBr): ν/cm^{-1} 3357, 2225, 1560, 1525, 1478, 1375, 1294, 1160.

Determination of pK_a by spectrophotometric pH titration

10^{-3} M stock solutions in DMSO of compounds **2a–2j** were prepared and kept in the dark in the fridge. 0.1 M NaCl–0.1 M HEPES buffer solutions were prepared by adjusting the pH to a given value with either 1 M HCl (for pH = 2 to 7.4) or 1 M NaOH (for pH 7.6 to 10). Titration solutions were prepared by mixing 20 μL of compound **2a–2j** stock solution, 500 μL DMSO to ensure total solubility and 2.0 mL of the buffered solution to obtain a final concentration of 8×10^{-6} M. The absorption spectrum of each batch was then recorded.

The variation of the absorbance A at the wavelength of the maximum absorption of the phenolate ($A_{max}^{ArO^-}$) was plotted as a function of pH. The sigmoid curve obtained was fitted using a least square nonlinear regression analysis according to eqn (1). The only adjustable parameter in eqn (1) was K_a.

The same experiment was done recording the emission of fluorescence. The excitation wavelength was set at the wavelength of the isosbestic point obtained in the absorption titration. Full titration data (absorption and emission) are given in Fig. 2, 3 and Fig. SI-1 to SI-8.†

Cellular confocal imaging at various pH values

Fluorescence imaging was performed using a Zeiss LSM510 confocal microscope and an argon laser at 488 nm for the excitation of compound **2a** and at 514 nm for the excitation of compound **2g**.

Light was reflected by a dichroic mirror (HFT488/561 for **2a** and 458/514 for **2g**), and directed toward the sample using an A-Plan 40× Zeiss objective (NA = 0.65). The emitted fluorescence was collected by the objective, passed through the dichroic mirror, a long-pass filter (490 nm for **2a** and **2g**) and an emission band-pass filter defining the "green" (500–550 nm for **2a** and 535–590 nm for **2g**) and "red" channels (600–650 nm for **2a** and 650–710 nm for **2g**) before the detector. Each fluorescence image is the average of four pictures and was recorded with the LSM5 software.

Cell culture. HeLa (ATCC-CL-2) cells were maintained in Dulbecco's Modified Eagle's medium (DMEM, Life Technologies, Courtaboeuf, France) supplemented with 10% fetal bovine serum (FBS, Life Technologies) and maintained at 37 °C with a 5% CO_2 atmosphere. Cells were seeded on Labtech (10 000 per chamber) 12 hours before experiment. Four hours before imaging, the medium was removed and replaced by DMEM without phenol red (Life Technologies) at an appropriate pH (*i.e.* 7.4, 7.2, 7 or 6.8). Probe **2a** or **2g** (1 μM) was added 1 minute before imaging, and fluorescence images were acquired without washing.

Notes and references

1 M. D. Liptak, K. C. Gross, P. G. Seybold, S. Feldgus and G. C. Shields, *J. Am. Chem. Soc.*, 2002, **124**, 6421–6427.
2 J. Han and K. Burgess, *Chem. Rev.*, 2010, **110**, 2709–2728.
3 I. Kurtz and R. S. Balaban, *Biophys. J.*, 1985, **48**, 499–508.
4 Z. Zhujun and W. R. Seitz, *Anal. Chim. Acta*, 1984, **160**, 47–55.
5 T. I. Rink, R. Y. Tsien and T. Pozzan, *J. Cell Biol.*, 1982, **95**, 189–196.
6 J. E. Whitaker, R. P. Haugland and F. G. Prendergast, *Anal. Biochem.*, 1991, **194**, 330–344.
7 Y. Yang, M. Lowry, X. Xu, J. O. Escobedo, M. Sibrian-Vazquez, L. Wong, C. M. Schowalter, T. J. Jensen, F. R. Fronczek, I. M. Warner and R. M. Strongin, *Proc. Natl. Acad. Sci. U. S. A.*, 2008, **105**, 8829–8834.
8 E. Nakata, Y. Nazumi, Y. Yukimachi, Y. Uto, H. Maezawa, T. Hashimoto, Y. Okamoto and H. Hori, *Bioorg. Med. Chem. Lett.*, 2011, **21**, 1663–1666.
9 C. Zhang, L. R. Dalton, M.-C. Oh, H. Zhang and W. H. Steier, *Chem. Mater.*, 2001, **13**, 3043–3050.
10 (*a*) K. A. Willets, O. Ostroverkhova, M. He, R. J. Twieg and W. E. Moerner, *J. Am. Chem. Soc.*, 2003, **125**, 1174–1175; (*b*) S. Y. Nishimura, S. J. Lord, L. O. Klein, K. A. Willets, M. He, Z. Lu, R. J. Twieg and W. E. Moerner, *J. Phys. Chem. B*, 2006, **110**, 8151–8157; (*c*) S. J. Lord, N. R. Conley, H.-l. D. Lee, R. Samuel, N. Liu, R. J. Twieg and W. E. Moerner, *J. Am. Chem. Soc.*, 2008, **130**, 9204–9205; (*d*) J. Bouffard, Y. Kim, Timothy M. Swager, R. Weissleder and S. A. Hilderbrand, *Org. Lett.*, 2008, **10**, 37–40; (*e*) S. J. Lord, N. R. Conley, H.-l. D. Lee, S. Y. Nishimura, A. K. Pomerantz, K. A. Willets, Z. Lu, H. Wang, N. Liu, R. Samuel, R. Weber, A. Semyonov, M. He, R. J. Twieg and W. E. Moerner, *ChemPhysChem*, 2009, **10**, 55–65; (*f*) X. Zhou, F. Su, Y. Tian, C. Youngbull, R. H. Johnson and D. R. Meldrum, *J. Am. Chem. Soc.*, 2011, **133**, 18530–18533.
11 (*a*) Y. Jin, Y. Tian, W. Zhang, S.-H. Jang, A. K.-Y. Jen and D. R. Meldrum, *Anal. Bioanal. Chem.*, 2010, **398**, 1375–1384; (*b*) Y.-A. Son, S.-Y. Gwon, S.-Y. Lee and S.-H. Kim, *Spectrochim. Acta, Part A*, 2010, **75**, 225–229.
12 E. Font-Sanchis, R. E. Galian, F. J. Céspedes-Guirao, Á. Sastre-Santos, L. R. Domingo, F. Fernández-Lázaro and J. Pérez-Prieto, *Phys. Chem. Chem. Phys.*, 2010, **12**, 7768–7771.
13 (*a*) D. Villemin and L. Liao, *Synth. Commun.*, 2001, **31**, 1771–1780; (*b*) S. Liu, M. A. Haller, H. Ma, L. R. Dalton, S.-H. Jang and A. K.-Y. Jen, *Adv. Mater.*, 2003, **15**, 603–607.
14 M. Baruah, W. Qin, N. Basarić, W. M. De Borggraeve and N. Boens, *J. Org. Chem.*, 2005, **70**, 4152–4157.
15 C. Hansch, A. Leo and R. W. Taft, *Chem. Rev.*, 1991, **91**, 165–195.
16 M. S. Baranov, K. A. Lukyanov, A. O. Borissova, J. Shamir, D. Kosenkov, L. V. Slipchenko, L. M. Tolbert, I. V. Yampolsky and K. M. Solntsev, *J. Am. Chem. Soc.*, 2012, **134**, 6025–6032.

17 A. Weller, *Z. Elektrochem.*, 1952, **56**, 662–668.
18 G. Koeckelberghs, S. Sioncke, T. Verbiest, A. Persoons and C. Samyn, *Polymer*, 2003, **44**, 3785–3794.
19 (*a*) N. Boens, W. Qin, N. Basarić, J. Hofkens, M. Ameloot, J. Pouget, J.-P. Lefèvre, B. Valeur, E. Gratton, M. vandeVen, N. D. J. Silva, Y. Engelborghs, K. Willaert, A. Sillen, A. J. W. G. Visser, A. van Hoek, J. R. Lakowicz, H. Malak, I. Gryczynski, A. G. Szabo, D. T. Krajcarski, N. Tamai and A. Miura, *Anal. Chem.*, 2007, **79**, 2137–2149; (*b*) K. Rurack and M. Spieles, *Anal. Chem.*, 2011, **83**, 1232–1242.